Electronic supplementary information (ESI) for

Gel polymer electrolytes based on single-ion conducting polyelectrolyte (SICP) and SICP-functionalized carbon nanotubes

*Yu-Hsuan Lu†, Kuan-Chun Wang† and Ying-Ling Liu**
Department of Chemical Engineering, National Tsing Hua University, No. 101, Sec. 2, Kuang-Fu Road, Hsinchu 300044, Taiwan.

† These 2 authors contribute equally to this article.
* Corresponding author, E-mail: liuyl@mx.nthu.edu.tw

Experimental part

Materials

CBSI was prepared in the laboratory according to the reported method.[S1] 4,4'-Oxydianiline (ODA), *tert*-butyl *α*-bromoisobutyrate (BiB), *N,N,N,N,N*-pentamethyldiethylenetriamine (PMDTA), and poly(vinylidene difluoride-co-hexafluoropropylene) (PVDF-HFP, molecular weight: about 400,000 Da) were purchased form Sigma-Aldrich. Pyridine, triphenyl phosphite (TPP), lithium chloride (LiCl), copper bromide (CuBr), ethylene carbonate (EC), and diethyl carbonate (DEC) were purchased from Alfa Aesar. Lithium hydroxide (LiOH) was purchased from Acros Organics. All reagents were used as received. Multiwalled carbon nanotubes (MWCNT) with diameters of 10-50 nm and lengths of 1-25 μm were received from Carbon Nanotube Co., Korea. *N*-methyl-2-pyrrolidone (NMP), tetrahydrofuran (THF), and methanol (MeOH) were received from TEDIA. Li metal foil (>99.9%) was purchased from UBIQ Technology Co., Ltd. The cathode electrodes were prepared in the laboratory by blending $LiFePO_4$ (LFP, UBIQ Technology Co., Ltd.), polyvinylidene difluoride (PVDF, Sigma Aldrich) binder, and Super P (UBIQ Technology Co., Ltd.) in a weight ratio of 8:1:1 in NMP solvent. The resulting slurry was cast onto aluminum foil (UBIQ Technology Co., Ltd.) and dried overnight at 80 °C under vacuum. The active material weight of the prepared cathode was approximately 2 mg cm^{-2}.

Synthesis of polyamide-based sulfonimide single-ion conductor (PASI)

PASI was synthesized by polymerization between of CBSI and ODA in an equimolar ratio. CBSI (0.57 g, 1.5 mmol) and ODA (0.3 g, 1.5 mmol) were dissolved in 5 mL NMP, followed by the addition of triphenyl phosphite (0.78 mL), pyridine (2.25 mL), and LiCl (0.28 g) as catalysts. The reaction was carried out under nitrogen at 100 °C for 24 h. The polymer was precipitated by adding 160 mL methanol to remove unreacted monomers. The resulting solid was collected and dried in a vacuum oven at 60 °C for 24 h, yielding a light brown powder with a yield of 95%. The obtained polymer was then dissolved in NMP and added dropwise to 0.1 M LiOH in methanol solution for ion exchange. The final yield of PASI was 75%.

Preparation of PASI-modified CNT (CNT-PASI)

BiB-modified MWCNT: (BiB) was first chemically bonded to MWCNTs via atom transfer radical addition. MWCNT (0.3 g), *tert*-butyl α-bromoisobutyrate (0.705 mL), PMDTA (0.083 mL), and CuBr (30 mg) were placed in a round-bottom-flask with 50 mL THF. After purged with argon for 30 minutes, the flask was frozen using liquid nitrogen and under vacuum before reacting at 60 °C for 24 h. The product was purified by centrifugation and washed extensively with THF to remove unreacted monomers and catalysts. The resulting product (MWCNT-BiB) was dried under vacuum at 60 °C for 24 h.

Hydrolysis of MWCNT-BiB: MWCNT-BiB (0.3 g) and KOH (1.7 g, 3.78 mmol) were reacted in 150 mL THF at room temperature for 48 h. After centrifugation, the solid was washed with 0.1 M HCl to exchange K^+ with H^+, then washed by extensive THF. The obtained MWCNT-COOH was dried under vacuum at 60 °C for 24 h.

Grafting PASI chains to MWCNT: CBSI and ODA (1:1 molar ratio) were dissolved in 5 mL NMP with triphenyl phosphite (0.78 mL), pyridine (2.25 mL), and LiCl (0.28 g). After adding MWCNT-COOH, the mixture was reacted at 100 °C for 24 h under nitrogen. The solid fraction was then collected by centrifugation and washed with NMP and THF to remove the physically absorbed PASI chains and reactants. The product was dispersed in 0.1 M LiOH methanol solution to exchange H^+ with Li^+, followed by washed with methanol and THF. The obtained product (MWCNT-PASI) was dried under vacuum at 60 °C for 24 h.

Preparation of gel polymer electrolytes

PVDF-HFP and PASI were dissolved in NMP at a 1:1 weight ratio (10 wt% solid content). The mixture was stirred for 24 h, filtered, and added with MWCNT-PPASI at different fractions (0 - 0.05 wt%). The solution was poured into a PDMS mold and dried under vacuum at 50 °C for 12 h, followed by 60 °C for 12 h and 80 °C for another 12 h for full removal of the solvent. The resulting films were cut into 19 mm discs and were then immersed in an EC/DMC (v:v = 1:1) mixture for further battery assembly in argon-filled glovebox. The prepared GPEs were labeled as GPE-PASI/CNT-X, X denoting to the weight percentages of MWCNT-PASI in the samples.

Instrumental and measurements methods

Fourier transform infrared (FTIR) spectra were obtained in the wavenumbers of 400 – 4000 cm^{-1} (PerkinElmer Spectrum Two). NMR spectra were obtained with BRUKER AVANCE 500 NMR instrument (500 MHz) using DMSO-d_6 as a solvent. Micro Raman Identify Dual instrument was utilized in recording the spectroscopies using a 633 nm laser as the radiation source to observe the Raman diffraction behavior of the sample. An X-ray photoelectron spectroscopy (XPS) instrument, PHI 5000 VersaProbe II (from ULVAC-PHI, Inc.), was employed in XPS analysis. High-resolution transmission electron microscopic (HRTEM) photographs were recorded with JEOL JEM-2010 HRTEM instrument. Thermogravimetric analysis (TGA) thermograms are recorded with a Thermal Analysis (TA) Co., TGA-Q50 instrument (heating rate: 10 °C min^{-1}; air stream: 100 mL min^{-1}). Differential scanning calorimetric (DSC) were analyzed with a TA DSC-Q20 at a heating rate of 10 °C min^{-1} and under a nitrogen stream of 50 mL min^{-1}.

The electrolyte uptake (η) was measured by the weighing method. The membranes were dried in a vacuum oven at 80 °C overnight to remove moisture. The initial dry weight (M_0) was recorded before immersing the membranes in EC/DMC (1:1 v/v). After 24 h, excess electrolyte was removed using a tissue, and the swollen weight (M_1) was recorded. The electrolyte uptake (η) was calculated using the ***Equation (1)***:

$$\eta = \frac{M_1 - M_0}{M_0} \times 100\ \% \quad (1)$$

Electrochemical measurements were carried out with an electrochemical instrument CHI 6081E from CH Instrument Co. The swelled membranes (GPE) were placed between two stainless steel electrodes (diameter: 15.5 mm) and assembled

into a CR2032 coin cell. The assembled cells were kept at 60 °C 12 h to improve interfacial contact. After cooling down to 25 °C the next day, electrochemical impedance spectroscopy (EIS) was conducted with 0.01 V over a frequency range of 1 MHz to 1 Hz. The bulk resistance (R) was determined from the Nyquist plot, and the ionic conductivity (σ) was calculated using the ***Equation (2)***:

$$\sigma = \frac{d}{R \times A} \qquad (2)$$

Where d and A represent the membrane thickness and effective area of the GPE, respectively.

For electronic conductivity, amperometric i-t curve method was used. The test was conducted under similar conditions as ionic conductivity measurements, with a fixed voltage applied to measure steady-state current. Resistance was obtained and substituted into the ionic conductivity formula to determine electronic conductivity.

Electrochemical stability was evaluated using linear sweep voltammetry (LSV). The electrolyte was sandwiched between a lithium metal electrode and a stainless steel electrode in a coin cell with a scan rate of 0.01 V s^{-1} from 2.5 V to 6 V.

The lithium transference number (t_{Li^+}) was determined using amperometric i-t curve and EIS methods. The symmetric cell was assembled with lithium metal electrodes and tested using a small polarization voltage (10 mV). Initial and steady-state currents (I_0 and I_S) as well as interfacial resistances before and after polarization (R_0 and R_S) were used to calculate t_{Li^+} by the ***Equation (3)***:

$$t_{Li}^{+} = \frac{I_s(\Delta V - R_0 I_0)}{I_0(\Delta V - R_s I_s)} \qquad (3)$$

Lithium plating−stripping galvanostatic cycling tests were carried out to assess the interface stability of GPE with symmetric lithium electrodes under various current densities at room temperature. Battery performance tests were conducted with $LiFePO_4$|GPE|Li batteries using BAT-750B instrument (AcuTech System Co.) with a voltage range of 2.5 to 4.0 V.

Tables discussed in the main text

***Table S1*.** Collected data in multiple measurements of ionic conductivities of GPE-PASI and GPE-PASI/CNT-0.02.

Measurements	R_b (Ω)	Ionic conductivities (10^{-5} S cm^{-1})
GPE-PASI (run 1)	416	1.15
GPE-PASI (run 2)	405	1.18
GPE-PASI (run 3)	500	1.07
GPE-PASI (run 4)	462	1.11
GPE-PASI/CNT-0.02 (run 1)	219	2.35
GPE-PASI/CNT-0.02 (run 2)	296	2.23
GPE-PASI/CNT-0.02 (run 3)	211	2.34
GPE-PASI/CNT-0.02 (run 4)	263	2.28
GPE-PASI/CNT-0.02 (run 5)	223	2.30

***Table S2*.** Collected data in multiple measurements of lithium transference numbers of GPE-PASI and GPE-PASI/CNT-0.02.

Measurements	ΔV (mV)	I_o (μA)	I_s (μA)	R_o (Ω)	R_s (Ω)	t_{Li^+}
GPE-PASI (run 1)	10	6.385	5.711	1213.5	1342.1	0.86
GPE-PASI (run 2)	10	6.616	6.125	1145.7	1189.1	0.83
GPE-PASI (run 3)	10	6.555	6.143	1194.9	1242.0	0.84
GPE-PASI/CNT-0.02 (run 1)	10	6.564	6.129	1290.1	1367.2	0.88
GPE-PASI/CNT-0.02 (run 2)	10	7.863	7.386	1026.4	1074.7	0.88
GPE-PASI/CNT-0.02 (run 3)	10	6.481	6.133	1334.6	1383.2	0.85

Table S3. Summary of performance of SICPE-based polymer electrolytes

SICPE-based GPEs [a]	Additive contents (wt%)	Ionic conductivity (mS cm^{-1})	t_{Li^+}	Cycles (capacity retention)	Reference
GPE-PASI/CNT-0.02	0.02	0.099 (25 °C)	0.87	400 (87.2 %)	This work
GPE-PAVM:TiO_2	6	4.5 (30 °C)	0.7	1000 (71 %)	[S2]
PPMBB10	10	1.03 (25 °C)	0.79	364 (76%)	[S3]
PMMA-IL-TFSI/LiTFSI	11	3.13 (25 °C)	0.96	500 (~90 %)	[S4]
ILGPE-15%-SiO2-PAA@Li	15	0.74 (25 °C)	0.48	100 (87 %)	[S5]
PC-NP20	20	0.095 (25 °C)	0.8	-	[S6]
$Li_{1.5}Al_{0.5}Ge_{1.5}(PO_4)_3$	30	0.83 (30 °C)	0.93	800 (99.8%)	[S7]
LiNPs40/S	40	0.017 (25 °C)	0.67	10 (~100 %)	[S8]

[a] Additive type: [S2] TiO_2 nanoparticle-decorated polymer framework comprising poly(acrylonitrile-co-vinyl acetate) blended with poly(methyl methacrylate); [S3] ionic liquid (IL)-decorated poly(methyl methacrylate) (PMMA) nanoparticles; [S4] core-shell structured SiO2 nanoparticles; [S5] fluorine-containing single-ion polymeric electrolyte: LiP(VDF-*co*-MAF)BB (Polyvinylidene fluoride trifluoromethyl acrylate lithium borate polymer; subsequently referred to as PPMBB); [S6] poly(methyl methacrylate) nanoparticles with a lithium sulfonamide surface functionality (LiPNP); [S7] $Li_{1.5}Al_{0.5}Ge_{1.5}(PO_4)_3$ nanoparticles alternated diblock lithiated bis(benzene sulfonyl)imide polyanion with repeating ether groups; [S8] methacrylic polymeric nanoparticles (NPs) functionalized with a lithium sulfonamide group.

Figures discussed in the main text.

Figure S1 showed the spectra for characterizing PASI. The structure of PASI was carried out using FTIR measurements. The characteristic absorption peaks of sulfonic acid groups from the CBSI precursor, attributed to S=O stretching (1161 cm^{-1} and 1321 cm^{-1}), were retained in PASI. Also, the original C=O stretching band of CBSI disappeared, and new peaks corresponding to the amide functionalities of PASI emerged, including C=O (1655 cm^{-1} and 1604 cm^{-1}), N–H (1533 cm^{-1}), and C–N (1410 cm^{-1}). In ^{1}H NMR characterization (***Figure S2***), PASI showed a distinct resonance peak at δ = 10.35 ppm (1H, O=C–N***H***–Ph) suggesting the formation of amide linkages. In

addition, the aromatic protons exhibited signals at δ = 7–8 ppm. Notably, the primary amine signal of the ODA monomer (δ = 5 ppm) and the hydroxyl proton of CBSI (δ = 13 ppm) were both absent, confirming the successful formation of the polyamide-based single-ion conducting polymer. ***Figure S3*** shows the GPC chromatogram of PASI.

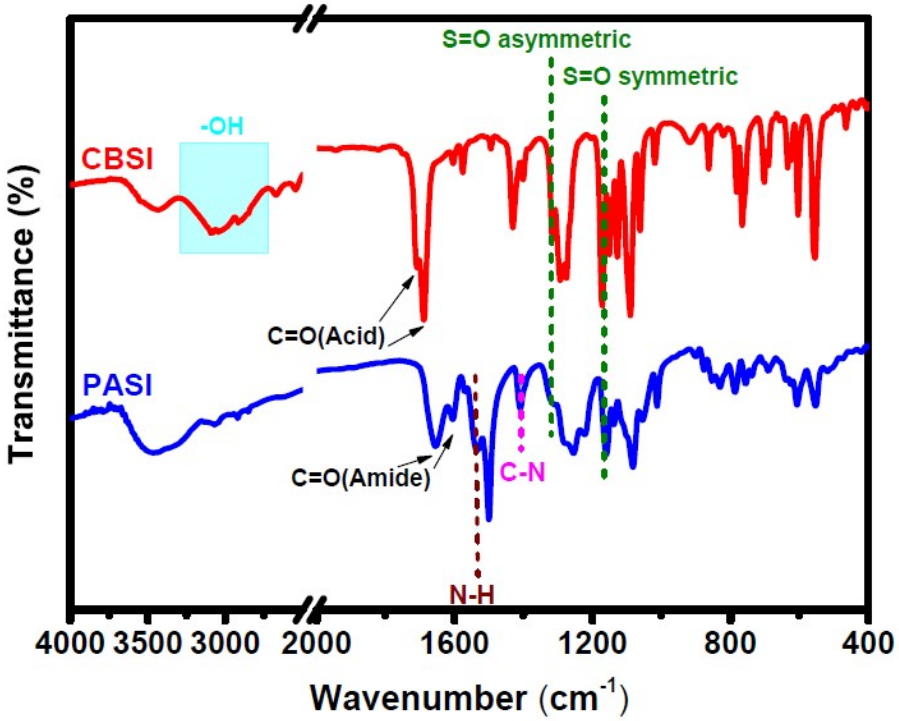

Figure S1. FTIR spectra of CBSI and PASI.

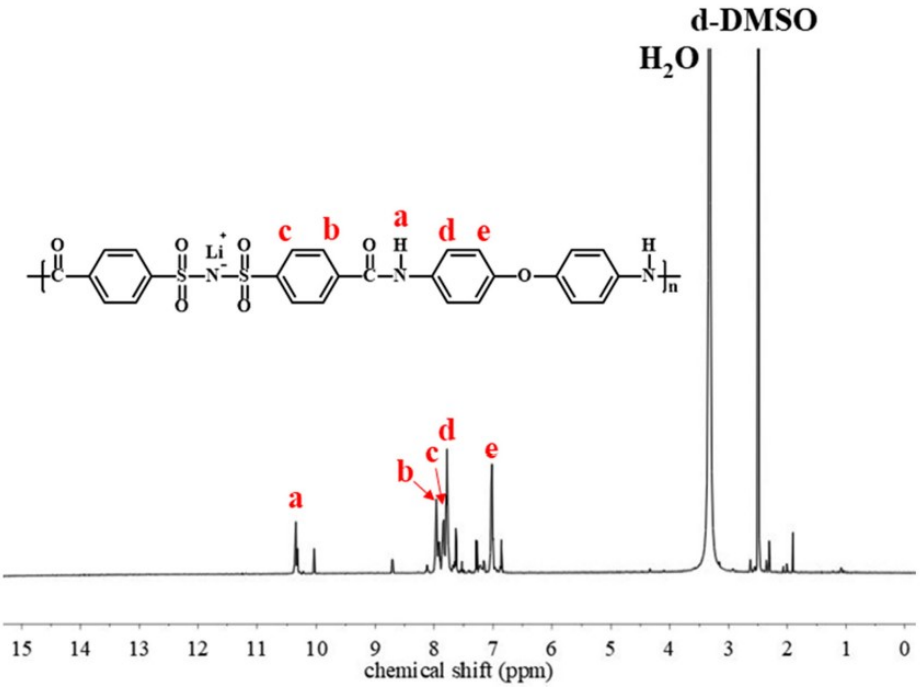

Figure S2. ^{1}H NMR spectrum of PASI.

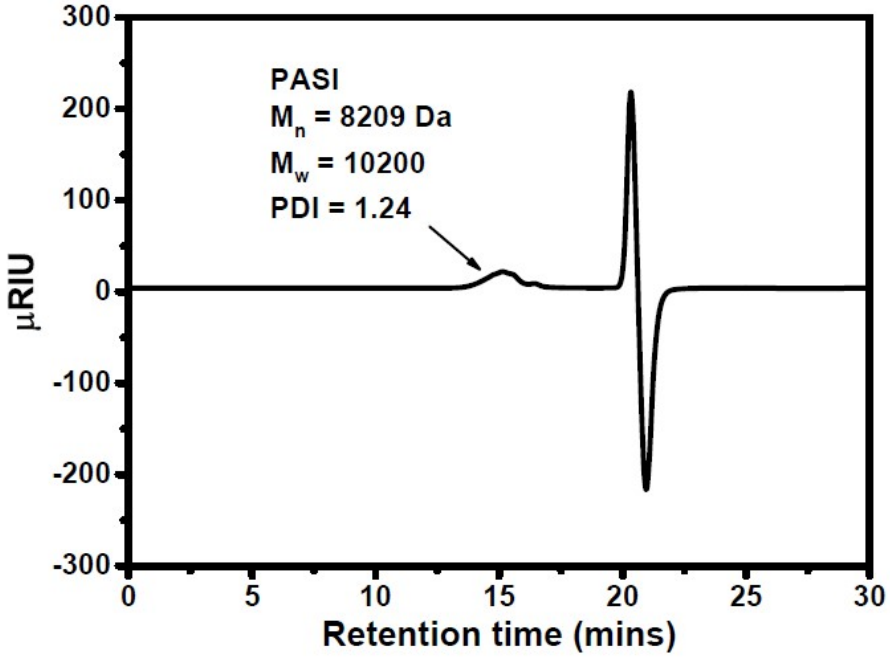

Figure S3. GPC chromatogram recorded on PASI.

The polymeric chain of PASI was further grafted on the surfaces of MWCNTs. Raman spectroscopy (***Figure S4***) was first employed to analyze the modified MWCNTs. Three prominent characteristic peaks were observed at 1338 cm^{-1}, 1573 cm^{-1}, and 2676 cm^{-1}. The peak at 1338 cm^{-1} corresponded to the disorder band (D-band), and the peak at 1573 cm^{-1} resulted from the in-plane stretching vibration of sp^2 carbon atoms (G-band). As chemical functionalization of MWCNTs introduced defects on their surfaces, reflecting an increase in D-band intensity, the degree of functionalization could be evaluated using the intensity ratio of the D-band over the G-band (D/G intensity ratio). As shown in ***Figure S4***, the D/G intensity ratio increased from 1.00 of pristine MWCNT to 1.08 after the modification with tert-butyl α-bromoisobutyrate (MWCNT-BiB) via atom transfer radical polymerization (ATRP), indicating successful grafting and increased structural defects. Subsequent reactions had minimal additional impact on defect formation, reflected by the relatively unchanged D/G ratio of MWCNT-COOH and MWCNT-PPASI (1.10 and 1.11, respectively). Additional Figures discussed in the main text are included below.

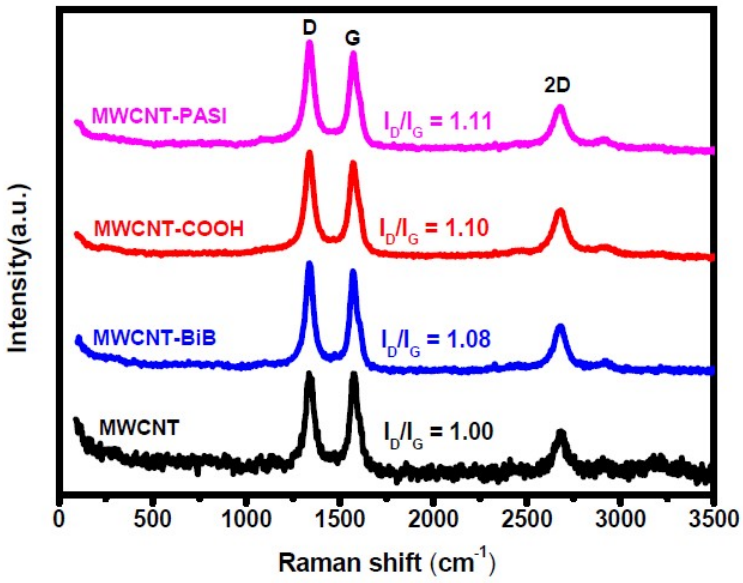

Figure S4. Raman spectra recorded on the products obtained at the process for surface-functionalization of MWCNTs.

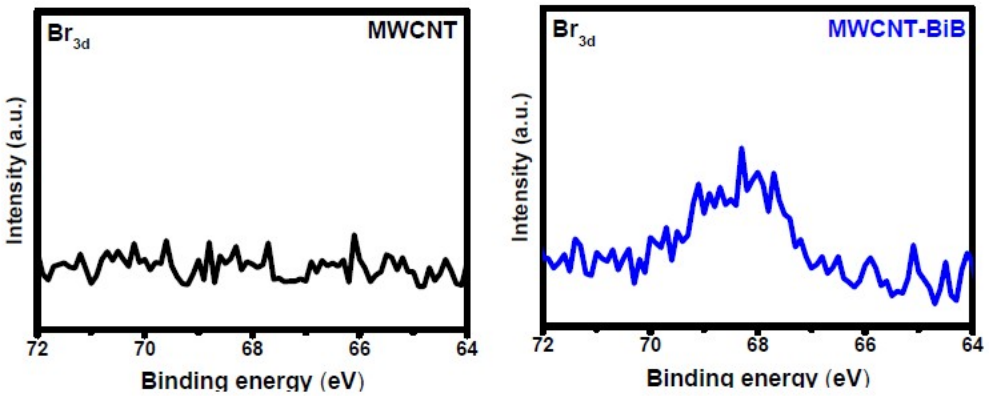

Figure S5. Br_{3d} core-level XPS spectra recorded on MWCNT and MWCNT-BiB.

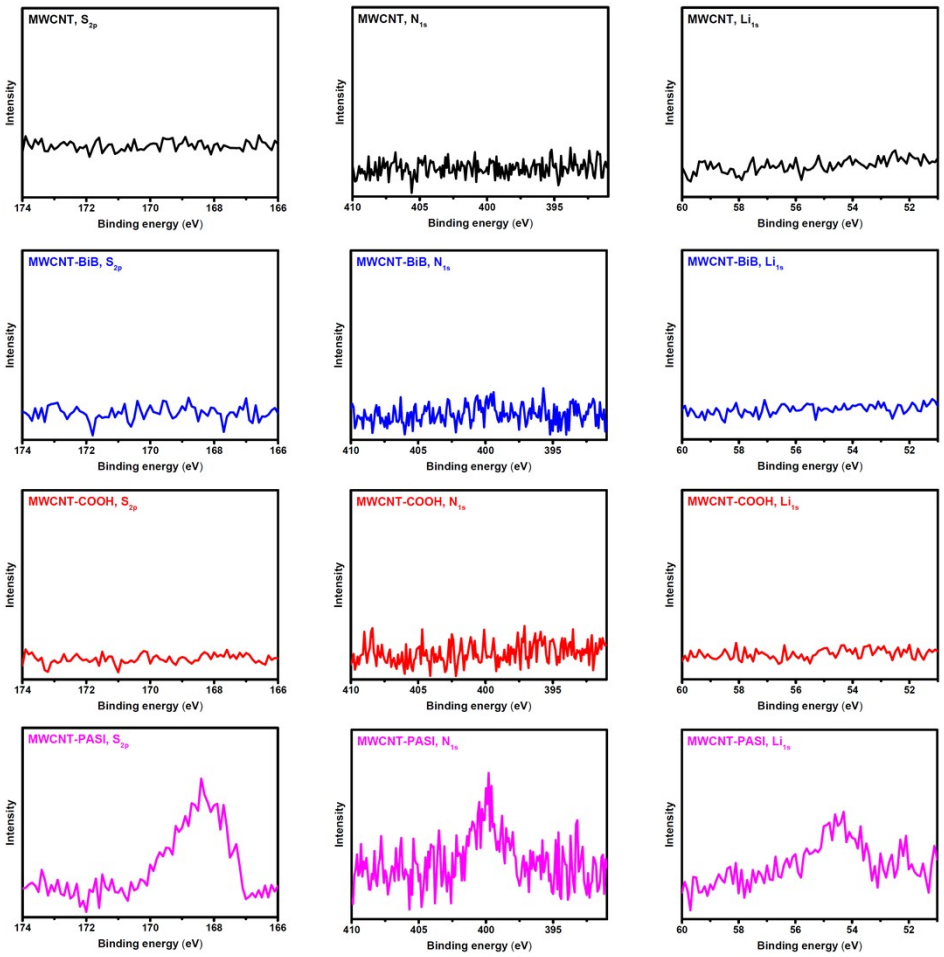

Figure S6. Elemental core-level XPS spectra recorded on the products obtained at the process for surface-functionalization of MWCNTs.

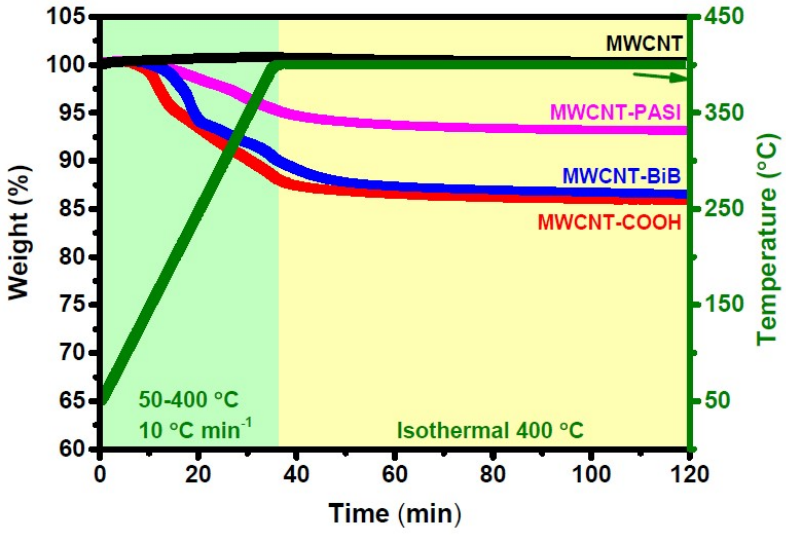

Figure S7. TGA thermograms recorded the products obtained at the process for

surface-functionalization of MWCNTs.

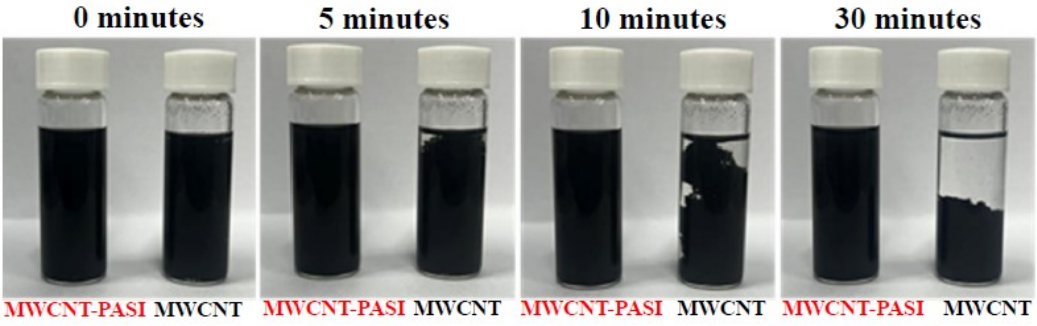

Figure S8. Photographs recorded on the solution of MWCNT and MWCNT-PASI in THF (0.1 wt%).

Figure S9. Photographs recorded on the prepared PASI/CNT-X nanocomposites, X denoting to the MWCNT-PASI contents in wt% of the nanocomposites.

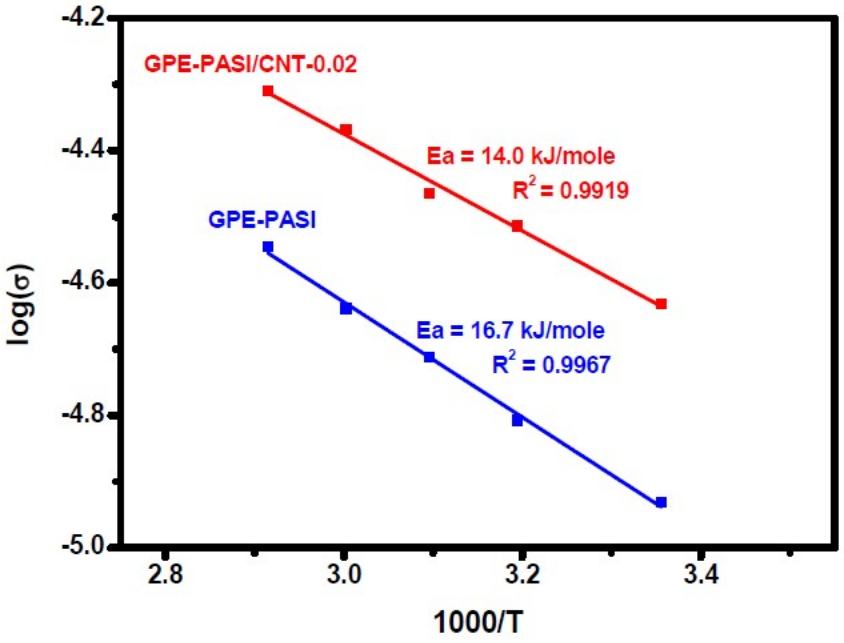

Figure S10. Arrhenius plots showing the relationships between the ionic conductivities and temperatures of GPE-PASI and GPE-PASI/CNT-0.02.

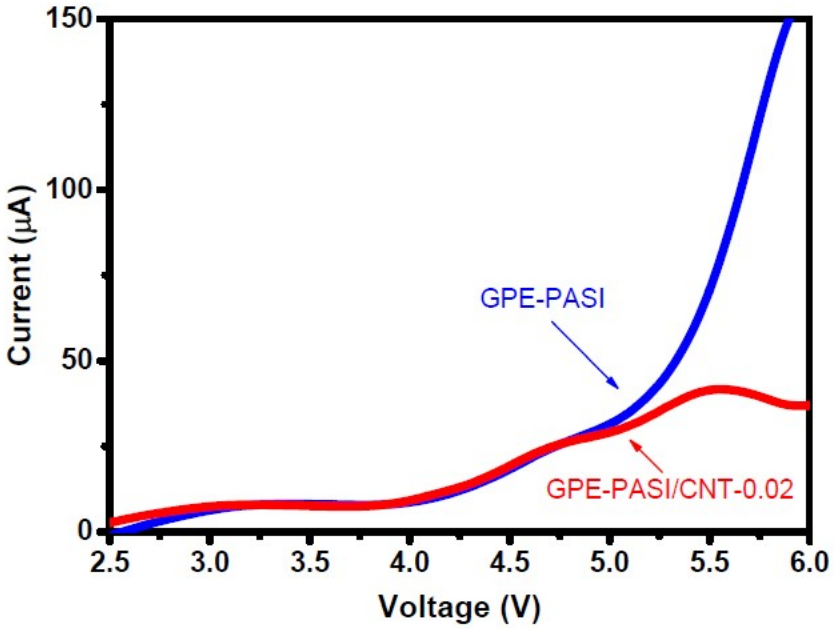

Figure S11. LSV curves recorded on GPE-PASI and GPE-PASI/CNT-0.02.

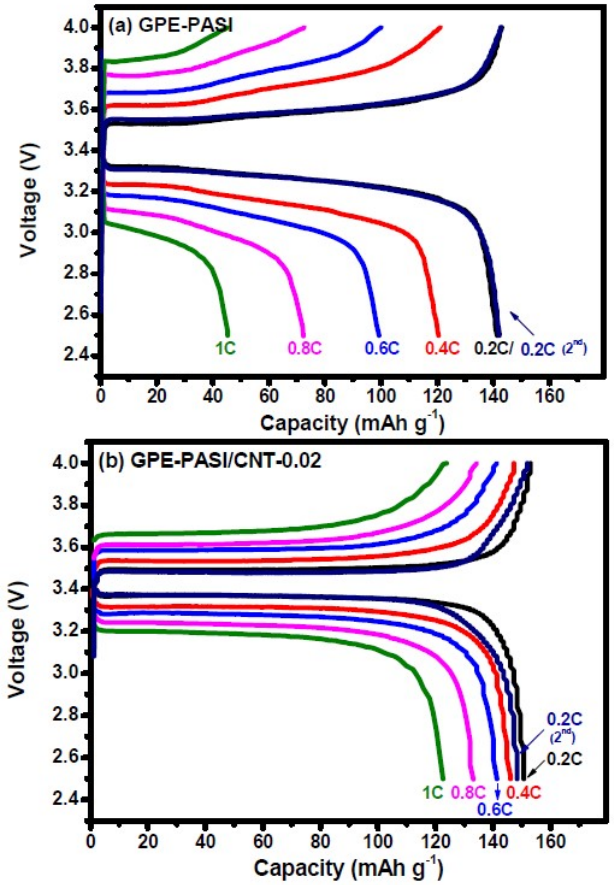

Figure S12. Charge−discharge curves recorded on GPE-PASI and GPE-PASI/CNT-0.02 at different C-rates.

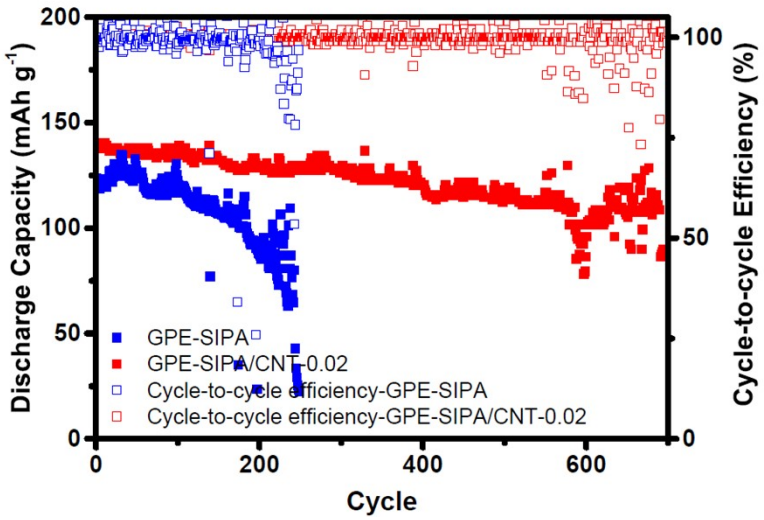

Figure S13. Discharge capacity and cycle-to-cycle efficiency recorded on the cells employing GPE-PASI and GPE-PASI/CNT-0.02 in the cycle tests at 0.5C.

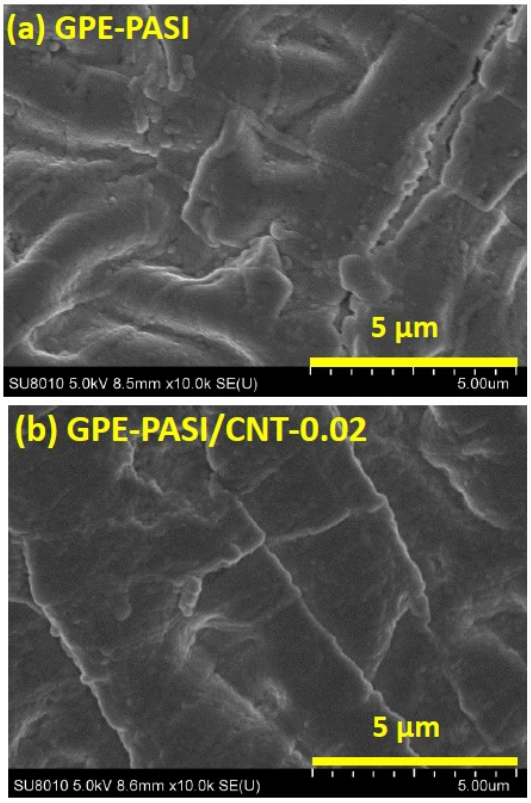

Figure S14. SEM micrographs recorded on GPE-PASI and GPE-PASI/CNT-0.02 after the cycling tests on the corresponding Li//Li symmetric cells at 0.2 mA cm^{-2}.

References

[S1] Y. Zhang, J. Ting, R. Rupesh, W. Cai, J. Li, G. Xu, Z. Chen, A. Lin and H. Cheng, *J. Mater. Sci.*, **2014**, 49, 3442-3450.

[S2] S. H. Wang, Y. Y. Lin, C. Y. Teng, Y. M. Chen, P. L. Kuo, Y. L. Lee, C. T. Hsieh and H. Teng, *ACS Appl. Mater. Interfaces,* **2016**, 8, 14776-14787.

[S3] Y. Yang, Y. Zhang, Y. Song, T. Ma, L. Zhang and S. Zhang, *Energies*, **2024**, 17, 3398.

[S4] Y. Li, K. W. Wong, Q. Dou and K. M. Ng, *J. Mater. Chem. A*, **2016**, 4, 18543-18550.

[S5] Q. Guo, Y. Han, H. Wang, W. Sun, H. Jiang, Y. Zhu, C. Zheng and K. Xie, *Electrochim. Acta*, **2018**, 288, 101-107.

[S6] L. Porcarelli, P. Sutton, V. Bocharova, R. H. Aguirresarobe, H. Zhu, N. Goujon, J. R. Leiza, A. Sokolov, M. Forsyth and D. Mecerreyes, *ACS Appl. Mater. Interfaces*, **2021**, 13, 54354-54362.

[S7] Y. Chen, C. Li, D. Ye, Y. Zhang, H. Bao and H. Cheng, *J. Membr. Sci.*, **2021**, 620, 118926.

[S8] A. Gallastegui, R. Del Olmo, M. Criado-Gonzalez, J. R. Leiza, M. Forsyth and D. Mecerreyes, *Small Sci.*, **2024**, 4, 2300235.